Chinese Journal of
POLYMER SCIENCE

RESEARCH ARTICLE

https://doi.org/10.1007/s10118-024-3133-5
Chinese J. Polym. Sci.

A Fluorine-Functionalized 3D Covalent Organic Framework with Entangled 2D Layers

Li-Bang Xiao[a,†], Zi-Han Wu[a,†], Jun-Jie Xin[b,†], Yuan-Peng Cheng[a], Bo Gui[a*], Jun-Liang Sun[b], and Cheng Wang[a*]

[a] *College of Chemistry and Molecular Sciences, Wuhan University, Wuhan 430072, China*
[b] *College of Chemistry and Molecular Engineering, Beijing National Laboratory for Molecular Sciences, Peking University, Beijing 100871, China*

Electronic Supplementary Information

Abstract Constructing three dimensional (3D) covalent organic frameworks (COFs) through the entanglement of two dimensional (2D) nets is a promising but underdeveloped strategy. Herein, we report the design and synthesis of a fluorine functionalized 3D COF (3D-An-COF-F) formed by entangled 2D **sql** nets. The structure of 3D-An-COF-F was determined by the combination of continuous rotation electron diffraction technique and modelling based on the chemical information from real space. Interestingly, compared to the isostructural 3D-An-COF without F atoms, 3D-An-COF-F showed an improved CO_2 sorption ability and higher CO_2/N_2 selectivity. Our study not only demonstrated the generality of constructing 3D COFs with entangled 2D nets by introducing bulky groups vertically in planar building blocks, but also will expand the diversity of 3D COFs for various applications.

Keywords 3D covalent organic frameworks; Fluorine; Entangled 2D layers; Electron diffraction; CO_2 adsorption

Citation: Xiao, L. B.; Wu, Z. H.; Xin, J. J.; Cheng, Y. P.; Gui, B.; Sun, J. L.; Wang, C. A fluorine-functionalized 3D covalent organic framework with entangled 2D layers. *Chinese J. Polym. Sci*. https://doi.org/10.1007/s10118-024-3133-5

INTRODUCTION

Covalent organic frameworks[1–4] (COFs) represent an emerging class of porous crystalline polymers constructed by covalently linked molecular building blocks following the principle of reticular chemistry.[5] Owing to their designable structures, low density, permanent porosity, and robust backbones, COFs have been found broad interest in catalysis,[6–10] adsorption and separation,[11–15] sensing,[16–19] optoelectronics,[20–23] energy,[24–27] and so on. Based on their structural characteristics, COFs can be mainly divided into either 2D COFs[28–32] or 3D COFs.[33–40] Structurally, 3D COFs can have abundant open channels and numerous open sites, which makes them promising for separation[41] and catalysis.[42] However, due to the challenging synthesis and structure determination,[33,34,43–45] far fewer 3D COFs have been reported. Consequently, many efforts have been devoted to diversifying the structures of 3D COFs. The most straightforward method to extend the structure pool of 3D COFs is to develop new 3D nodes suitable for constructing these structures. Thanks to worldwide efforts, polyhedral nodes with 4, 6 or 8 connectivity have been developed.[46–53] Unfortunately, the synthesis and structure determination of 3D COFs becomes more challenging as the valence of building blocks increases. Therefore, it is highly appealing to develop other strategies to construct 3D COFs.

Alternatively, it is also possible to construct 3D COFs from the entanglement of 2D planar sheets based on reticular chemistry.[54] For example, Yaghi and coworkers reported two 3D COFs composed of 2D layers constructed based on a distorted tetrahedral building block.[55] This work strongly confirms the possibility to construct 3D COFs through the entanglement of 2D layered nets, but very few examples have been successfully reported so far.[55–57] Very recently, we developed a new strategy to construct 3D COFs formed by 2D laminated sheets *via* the introduction of bulky hindrance to the vertical direction of planar building blocks.[56] However, the universality of this strategy should be further verified. In addition, the effect of pore environment modification on the properties of these 3D COFs with entangled structures is unknown.

Herein, we report the design and synthesis of a novel 3D COF formed by entangled 2D layers. The F atoms substituent precursor with bulky anthracene in the vertical direction was designed and synthesized. After further Schiff-base reaction, a novel 3D COF (3D-An-COF-F) was isolated, which is isostructural to our previously reported 3D-An-COF.[56] Based on the combination of continuous rotation electron diffraction (cRED) technique[36,58] and modelling with the chemical information in real space, 3D-An-COF-F was determined to be a 3D

* Corresponding authors, E-mail: guib09@whu.edu.cn (B.G.)
E-mail: chengwang@whu.edu.cn (C.W.)

† These authors contributed equally to this work.

We dedicated this work to Professor Jean-Pierre Sauvage on the occasion of his 80th birthday.

Received March 1, 2024; Accepted March 25, 2024; Published online May 10, 2024

framework entangled by two sets of nearly vertical 2D **sql** nets. Interestingly, 3D-An-COF-F showed enhanced CO_2 sorption performance and higher CO_2/N_2 selectivity compared to the reported 3D-An-COF. Therefore, it is general to construct 3D COFs with entangled 2D sheets from the planar building blocks with bulky groups in the vertical direction. This study also advances the design and synthesis of 3D COFs with entangled 2D layers for target applications in the future.

EXPERIMENTAL

General Considerations

3,5-Difluoro-4-formylphenylboronic acid (98%), palladium tetrakis(triphenylphosphine) (99%), and 1,2-difluorobenzene (98%) were purchased from Shanghai Aladdin Biochemical Technology Co., Ltd. 1,4-Dioxane (99%), acetic acid (99.5%), potassium carbonate (99%) and dichloromethane (99%) were obtained from Sinopharm Chemical Reagent Co., Ltd. All chemicals were used as received unless otherwise indicated. Deionized water was used in all experiments.

Synthesis of PADC-F

The N^9,N^9,N^{10},N^{10}-tetrakis(4-bromophenyl)-9,10-anthracene diamine was synthesized following previously reported procedure.[56] 3,5-Difluoro-4-formylphenylboronic acid (3.72 g, 20.00 mmol), N^9,N^9,N^{10},N^{10}-tetrakis(4-bromophenyl)-9,10-anthracenediamine (3.50 g, 4.00 mmol), palladium tetrakis(triphenylphosphine) (0.23 g, 0.20 mmol) and potassium carbonate (4.42 g, 32.00 mmol) were added to a flask containing 150 mL of 1,4-dioxane and 30 mL of water. The mixture was heated at 120 °C under nitrogen atmosphere for 3 days. After cooling down to room temperature, the solvents were removed under reduced pressure. Then the residues were purified by column chromatography [SiO_2:CH_2Cl_2/PE (2:1→ 5:1)] to yield PADC -F as a yellow solid (2.70 g, 63% yield). ^{1}H-NMR (400 MHz, $CDCl_3$, δ, ppm): 10.34 (s, 4H), 8.21–8.15 (m, 4H), 7.52 (d, J=8.8 Hz, 8H), 7.50–7.40 (m, 4H), 7.27 (s, 4H), 7.25 (s, 4H), 7.16 (d, J=10.1 Hz, 8H). ^{1}H-NMR (400 MHz, DMSO-d_6, δ, ppm): 10.19 (s, 4H), 8.20–8.15 (m, 4H), 7.83 (d, J=8.9 Hz, 8H), 7.59 (d, J=10.8 Hz, 12H), 7.23 (d, J=8.9 Hz, 8H). ^{13}C-NMR (100 MHz, $CDCl_3$, δ, ppm): 184.3, 162.3, 148.8, 148.5, 136.9, 131.6, 131.0, 128.5, 127.9, 124.8, 121.0, 110.1, 109.8. ^{19}F-NMR (376 MHz, $CDCl_3$, δ, ppm): −114.2. HR-MS (MALDI-TOF): m/z calcd. for $C_{66}H_{36}F_8N_2O_4$: 1072.2547 $[M]^+$; found: 1072.2552 $[M]^+$.

Synthesis of PADA

N^9,N^9,N^{10},N^{10}-tetraphenylanthracene-9,10-diamine (PADA) was synthesized following previously reported procedure.[56]

Synthesis of 3D-An-COF-F

To obtain high quality crystalline samples, we have tried hundreds of reaction conditions by changing solvents, temperature, and the concentration of acid (Fig. S1 in the electronic supplementary information, ESI). Finally, the optimized synthetic condition for the synthesis of 3D-An-COF-F was obtained as follows: A Pyrex tube was charged with PADA (8.8 mg, 0.01 mmol), PADC-F (10.7 mg, 0.01 mmol), 1,2-difluorobenzene (0.30 mL) and 9 mol/L aqueous acetic acid (0.1 mL). After being degassed by freeze-pump-thaw technique for three times and then sealed under vacuum, the tube was placed in an oven at 120 °C for 3 days. The resulting precipitate was filtered, washed with DMF, tetrahydrofuran and dichloromethane for 2 days, dried at 100 °C under vacuum for 12 h. The activated 3D-An-COF-F was obtained as a yellow powder (11.0 mg, 59% yield). Elemental analysis for the calculated: C, 76.03%; H, 3.77%; N, 7.19%. Found: C, 76.43%; H, 4.14%; N, 5.35%.

Synthesis of 3D-An-COF

3D-An-COF was synthesized following previously reported procedure.[56]

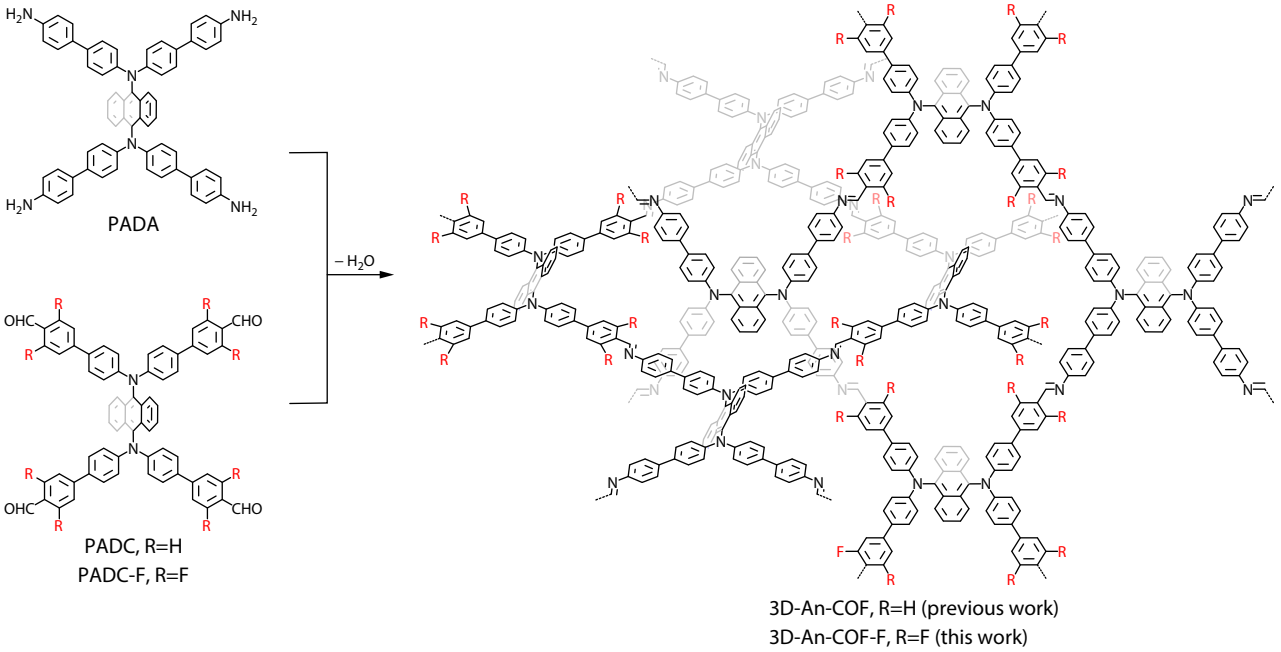

Scheme 1 Construction of 3D-An-COF and 3D-An-COF-F from the molecular precursors.

https://doi.org/10.1007/s10118-024-3133-5

RESULTS AND DISCUSSION

To construct 3D COFs composed of entangled 2D nets with modified pore environment, we followed our previously developed strategy (Scheme 1) and designed a novel precursor N^9,N^9,N^{10},N^{10}-tetrakis(3',5'-difluoro-4'-carbaldehyde-[1,1'-biphenyl]-4-yl)anthracene-9,10-diamine (PADC-F). Then we tried to construct the 3D COF by reacting PADC-F with the reported N^9,N^9,N^{10},N^{10}-tetrakis(4′-amino-[1,1′-biphenyl]-4-yl)-anthracene-9,10-diamine (PADA)[56] (Scheme S2 in ESI). After plenty of trials to screen the reaction conditions about solvents/catalyst types and ratios (Fig. S1 in ESI), a highly crystalline yellow powder (3D-An-COF-F) was isolated by placing the precursors in the solvent mixture of 1,2-difluorobenzene/9 mol/L aqueous acetic acid (3:1, *V*:*V*) at 120 °C for 3 days (Fig. S2 in ESI). The atomic level of the covalent bond information in 3D-An-COF-F was characterized by Fourier transform infrared (FTIR) and solid-state NMR (ss-NMR) spectroscopies. A stretching bond at 1631 cm^{-1} in the FTIR spectrum (Fig. S3 in ESI) and a characteristic signal at 161 ppm in the ssNMR spectrum (Fig. S4 in ESI) can be observed, demonstrating the formation of imine bond. According to the scanning electron microscopy (SEM) image (Fig. S5 in ESI), 3D-An-COF-F displays a regular polyhedron morphology. Furthermore, thermogravimetric analysis (TGA) shows that 3D-An-COF-F exhibits high thermal stability and begins to decompose at ~450 °C (Fig. S6 in ESI). Moreover, 3D-An-COF-F shows good chemical stability in different solvents, including 0.1 mol/L HCl and 12 mol/L NaOH aqueous solution (Fig. S7 in ESI). In addition, 3D-An-COF-F exhibits a strong yellow fluorescence in the solid state (Fig. S9 in ESI).

The crystallinity of 3D-An-COF-F was investigated by powder X-ray diffraction (PXRD) experiment. As shown in Fig. 1(a), 3D-An-COF-F displays many intense and sharp diffraction peaks, demonstrating its excellent crystallinity. Considering the small size of the microcrystals (Fig. S5 in ESI), we then used continuous rotation electron diffraction (cRED) tech-

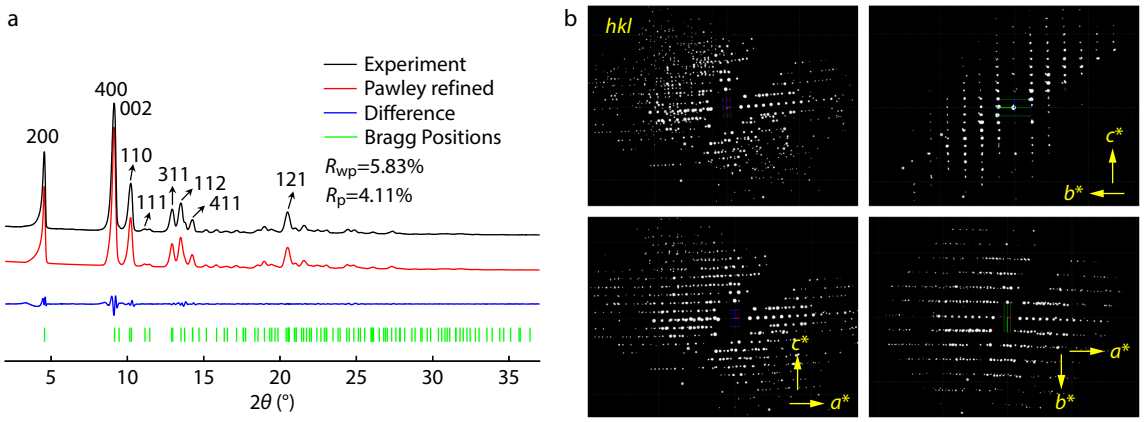

Fig. 1 Structure determination of 3D-An-COF-F. (a) The observed PXRD pattern (black), the Pawley refinement pattern (red), their difference (blue), the Bragg position from the modelled structure (green); (b) Reconstructed 3D reciprocal lattice of 3D-An-COF-F view from a^*, b^*, c^*.

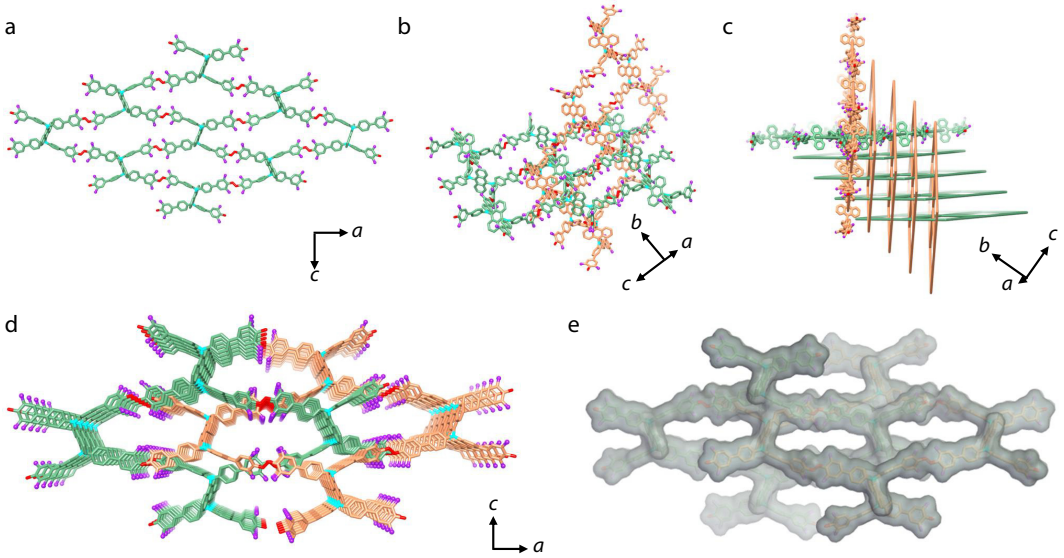

Fig. 2 Structure representation of 3D-An-COF-F. (a) Selected one layer of the 2D **sql** network; (b) Selected two entangled square nets; (c) Two sets of entangled square nets from different directions; (d) The porous network of 3D-An-COF-F; (e) Network surface of 3D-An-COF-F. The purple balls in the structures are F atoms.

https://doi.org/10.1007/s10118-024-3133-5

nique[58] to solve the crystal structure of 3D-An-COF-F (Fig. 1b). The cRED data for 3D-An-COF-F was collected in the low-dose mode at −174 °C and the resolution of data reached up to 1.4 Å. After reconstructing the 3D reciprocal lattice using REDp data processing software,[59] the unit cell of 3D-An-COF-F was determined as an orthorhombic *P* lattice with *a*=38.68 Å, *b*=8.86 Å, *c*=18.33 Å. Furthermore, 3D-An-COF-F shows almost the same PXRD peak positions (Fig. S10 in ESI) with our reported 3D-An-COF,[56] which is composed of entangled 2D sheets based on atomic resolution cRED data. Consequently, 3D-An-COF-F is isostructural to 3D-An-COF and a 3D structure model based on *Pccn* space group was built. Pawley refinement was subsequently conducted on the structure model, which gave a refined profile matched well with the observed pattern (Fig. 1a and see Tables S1 and S2 in ESI for details).

Based on the above results, 3D-An-COF-F consists of entangled 2D layered nets (Fig. 2). The steric anthracene was extended out of the **sql** sheets (Fig. 2a) connected by the molecular building blocks, which makes it difficult to stack the layers to form a 2D COF. Consequently, the 2D layers in the directions of **2***b*+*c* and **2***b*–*c* entangled with each other to give the 3D structure of 3D-An-COF-F (Fig. 2b). The distance between the layers in the same directions is about 0.66 nm (Fig. 2c) and the entanglement of these 2D layers produces a pore along the *b* axis (Fig. 2d). The permanent porosity of 3D-An-COF-F was evaluated by nitrogen (N_2) sorption isotherm at −196 °C. As can be seen in Fig. 3, 3D-An-COF-F has a typical type I isotherm, indicating its microporous structure. The Brunauer-Emmett-Teller (BET) surface area of 3D-An-COF-F was calculated to be 930 $m^2 \cdot g^{-1}$, which was close to our reported 3D-An-COF.[56] Moreover, the pore size distribution of 3D-An-COF-F was calculated by using a quenched solid density functional theory (QSDFT), which gave a narrow distribution centred at 0.55 nm, consistent with the measured value of the crystal structure.

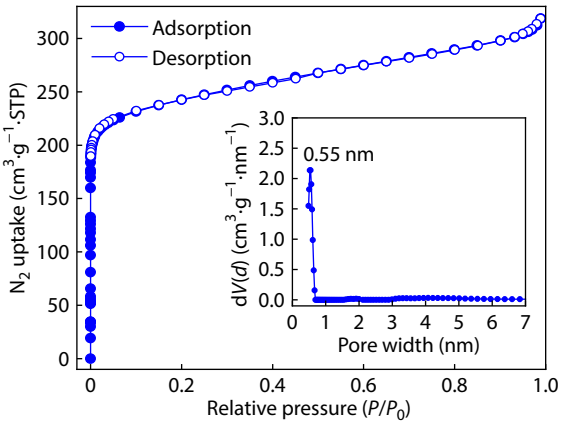

Fig. 3 N_2 sorption isotherm of 3D-An-COF-F at −196 °C and its pore size distribution.

Considering the microporous channels of 3D-An-COF-F were decorated by exposed F atoms, we hypothesized 3D-An-COF-F has the potential to be used in gas separation. As a proof-of-concept study, we then explored its CO_2/N_2 separation, as the capture of CO_2 from flue gas is vital in combating climate changes. The CO_2 and N_2 isotherms of 3D-An-COF-F and 3D-An-COF were conducted. Notably, both 3D-An-COF-F and 3D-An-COF showed reasonable CO_2 adsorption but negligible N_2 sorption at 0 °C (Fig. 4a). In addition, 3D-An-COF-F showed higher CO_2 uptake at both 0.01 and 0.1 MPa (Fig. 4b), indicating the enhanced CO_2 sorption ability compared to 3D-An-COF. The ideal adsorbed solution theory (IAST) was subsequently applied to calculate the adsorption selectivity for CO_2/N_2 mixture (15/85) of these two 3D COFs as a func-

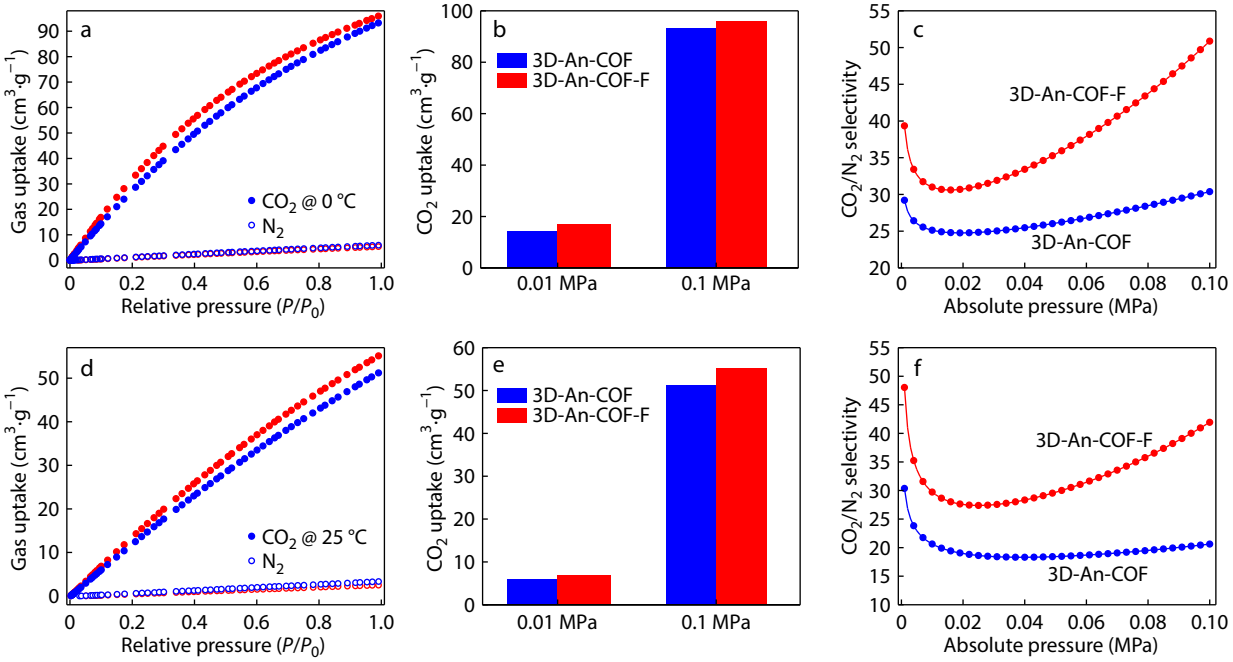

Fig. 4 CO_2 (solid circle) and N_2 (open circle) sorption isotherms of the 3D-An-COF (blue), 3D-An-COF-F (red) at (a) 0 °C and (d) 25 °C; CO_2 adsorption capacity at (b) 0 °C and (e) 25 °C; CO_2/N_2 selectivity of 3D-An-COF (blue), 3D-An-COF-F (red) at a ratio of 15/85 at (c) 0 °C and (f) 25 °C.

https://doi.org/10.1007/s10118-024-3133-5

tion of pressure. As we expected, 3D-An-COF-F showed a selectivity of 51 at 0 °C and 0.1 MPa (Fig. 4c), which was significantly higher than 3D-An-COF (30, 0 °C and 0.1 MPa). To evaluate the potential applications at ambient conditions, the sorption experiments was also carried out at 25 °C. As shown in Figs. 4(d) and 4(e), 3D-An-COF-F also exhibited higher CO_2 uptake at both 0.01 and 0.1 MPa. The CO_2/N_2 selectivity of 3D-An-COF-F at 25 °C and 0.1 MPa was twice of that for 3D-An-COF (21, 0.1 MPa, Fig. 4f). Based on these CO_2 sorption isotherms, the calculated isosteric heats of adsorption (Q_{st}) value of 3D-An-COF-F (30.6 kJ·mol^{-1}) was higher than that of 3D-An-COF (26.4 kJ·mol^{-1}) (Fig. S11 and Table S3 in ESI). As a result, the microporous 3D-An-COF-F with exposed F atoms displays significantly higher CO_2 sorption ability and CO_2/N_2 selectivity.

CONCLUSIONS

In conclusion, we designed and synthesized a fluorescent fluorine-functionalized 3D COF (3D-An-COF-F). According to the structure analysis, 3D-An-COF-F was formed by two sets of entangled 2D layers. Interestingly, 3D-An-COF-F displays enhanced CO_2 sorption ability and higher CO_2/N_2 selectivity to our previously reported 3D-An-COF without F atoms, demonstrating the modification of the pore environment by introducing F atoms. Therefore, it is general to construct 3D COFs formed by entangled 2D layers from the building blocks with bulky steric hindrance in the vertical direction and it will definitely inspire us to design other functional 3D COFs for target applications in the future.

Conflict of Interests

The authors declare no interest conflict.

Electronic Supplementary Information

Electronic supplementary information (ESI) is available free of charge in the online version of this article at http://doi.org/10.1007/s10118-024-3133-5.

Data Availability Statement

The data that support the findings of this study are available from the corresponding author upon reasonable request. The authors' contact information: chengwang@whu.edu.cn (C.W.), guib09@whu.edu.cn (B.G.).

ACKNOWLEDGMENTS

This work was financially supported by the National Natural Science Foundation of China (Nos. 22225503, U21A20285 and 22375153), the Hubei Provincial Natural Science Foundation of China (No. 2023AFA011) and the Fundamental Research Funds for Central Universities (No. 2042023kf0127). We also thank the Core Facility of Wuhan University.

REFERENCES

1 Ding, S. Y.; Wang, W. Covalent organic frameworks (COFs): from design to applications. *Chem. Soc. Rev.* **2013**, *42*, 548–568.
2 Diercks, C. S.; Yaghi, O. M. The atom, the molecule, and the covalent organic framework. *Science* **2017**, *355*, eaal1585.
3 Geng, K.; He, T.; Liu, R.; Dalapati, S.; Tan, K. T.; Li, Z.; Tao, S.; Gong, Y.; Jiang, Q.; Jiang, D. Covalent organic frameworks: design, synthesis, and functions. *Chem. Rev.* **2020**, *120*, 8814–8933.
4 Gui, B.; Ding, H.; Cheng, Y.; Mal, A.; Wang, C. Structural design and determination of 3D covalent organic frameworks. *Trends Chem.* **2022**, *4*, 437–450.
5 Yaghi, O. M.; Kalmutzki, M. J.; Diercks, C. S. in *Introduction to reticular chemistry: metal-organic frameworks and covalent organic frameworks*. John Wiley & Sons, Weinheim, Germany **2019**, pp. 1–494.
6 Zhi, Q.; Liu, W.; Jiang, R.; Zhan, X.; Jin, Y.; Chen, X.; Yang, X.; Wang, K.; Cao, W.; Qi, D.; Jiang, J. Piperazine-linked metalphthalocyanine frameworks for highly efficient visible-light-driven H_2O_2 photosynthesis. *J. Am. Chem. Soc.* **2022**, *144*, 21328–21336.
7 Yuan, C.; Fu, S.; Kang, X.; Cheng, C.; Jiang, C.; Liu, Y.; Cui, Y. Mixed-linker chiral 2D covalent organic frameworks with controlled layer stacking for electrochemical asymmetric catalysis. *J. Am. Chem. Soc.* **2024**, *146*, 635–645.
8 Yang, S.; Hu, W.; Zhang, X.; He, P.; Pattengale, B.; Liu, C.; Cendejas, M.; Hermans, I.; Zhang, X.; Zhang, J.; Huang, J. 2D Covalent organic frameworks as intrinsic photocatalysts for visible light-driven CO_2 reduction. *J. Am. Chem. Soc*. **2018**, *140*, 14614–14618.
9 Yao, L.; Rodríguez-Camargo, A.; Xia, M.; Mücke, D.; Guntermann, R.; Liu, Y.; Grunenberg, L.; Jiménez-Solano, A.; Emmerling, S. T.; Duppel, V.; Sivula, K.; Bein, T.; Qi, H.; Kaiser, U.; Grätzel, M.; Lotsch, B. V. Covalent organic framework nanoplates enable solution-processed crystalline nanofilms for photoelectrochemical hydrogen evolution. *J. Am. Chem. Soc.* **2022**, *144*, 10291–10300.
10 Wang, G. B.; Wang, Y. J.; Kan, J. L.; Xie, K. H.; Xu, H. P.; Zhao, F.; Wang, M. C.; Geng, Y.; Dong, Y. B. Construction of covalent organic frameworks *via* a visible-light-activated photocatalytic multicomponent reaction. *J. Am. Chem. Soc.* **2023**, *145*, 4951–4956.
11 Zhang, Z.; Kang, C.; Peh, S. B.; Shi, D.; Yang, F.; Liu, Q.; Zhao, D. Efficient adsorption of acetylene over CO_2 in bioinspired covalent organic frameworks. *J. Am. Chem. Soc.* **2022**, *144*, 14992–14996.
12 Fan, H.; Mundstock, A.; Feldhoff, A.; Knebel, A.; Gu, J.; Meng, H.; Caro, J. Covalent organic framework covalent organic framework bilayer membranes for highly selective gas separation. *J. Am. Chem. Soc.* **2018**, *140*, 10094–10098.
13 Khan, N. A.; Zhang, R.; Wu, H.; Shen, J.; Yuan, J.; Fan, C.; Cao, L.; Olson, M. A.; Jiang, Z. Solid-vapor interface engineered covalent organic framework membranes for molecular separation. *J. Am. Chem. Soc.* **2020**, *142*, 13450–13458.
14 Li, J.; Cheng, Z.; Wang, Z.; Dong, J.; Jiang, H.; Wang, W.; Zou, X.; Zhu, G. Ultramicroporous covalent organic framework nanosheets with functionality pair for membrane C_2H_2/C_2H_4 separation. *Angew. Chem. Int. Ed.* **2023**, *62*, e202216675.
15 Zeng, Y.; Zou, R.; Zhao, Y. Carbon dioxide capture: covalent organic frameworks for CO_2 capture. *Adv. Mater.* **2016**, *28*, 2855–2873.
16 Meng, Z.; Mirica, K. A. Covalent organic frameworks as multifunctional materials for chemical detection. *Chem. Soc. Rev.* **2021**, *50*, 13498–13558.
17 Jhulki, S.; Evans, A. M.; Hao, X. L.; Cooper, M. W.; Feriante, C. H.; Leisen, J.; Li, H.; Lam, D.; Hersam, M. C.; Barlow, S.; Brédas, J. L.; Dichtel, W. R.; Marder, S. R. Humidity sensing through reversible isomerization of a covalent organic framework. *J. Am. Chem. Soc.* **2020**, *142*, 783–791.

18 Das, G.; Biswal, B. P.; Kandambeth, S.; Venkatesh, V.; Kaur, G.; Addicoat, M.; Heine, T.; Verma, S.; Banerjee, R. Chemical sensing in two dimensional porous covalent organic nanosheets. *Chem. Sci.* **2015**, *6*, 3931–3939.

19 Hamzehpoor, E.; Ruchlin, C.; Tao, Y.; Liu, C. H.; Titi, H. M.; Perepichka, D. F. Efficient room-temperature phosphorescence of covalent organic frameworks through covalent halogen doping. *Nat. Chem.* **2023**, *15*, 83–90.

20 Xing, G.; Zheng, W.; Gao, L.; Zhang, T.; Wu, X.; Fu, S.; Song, X.; Zhao, Z.; Osella, S.; Martínez-Abadía, M.; Wang, H. I.; Cai, J.; Mateo-Alonso, A.; Chen, L. Nonplanar rhombus and kagome 2D covalent organic frameworks from distorted aromatics for electrical conduction. *J. Am. Chem. Soc.* **2022**, *144*, 5042–5050.

21 Jin, E.; Asada, M.; Xu, Q.; Dalapati, S.; Addicoat, M. A.; Brady, M. A.; Xu, H.; Nakamura, T.; Heine, T.; Chen, Q.; Jiang, D. Two-dimensional sp^2 carbon-conjugated covalent organic frameworks. *Science* **2017**, *357*, 673–676.

22 Jakowetz, A. C.; Hinrichsen, T. F.; Ascherl, L.; Sick, T.; Calik, M.; Auras, F.; Medina, D. D.; Friend, R. H.; Rao, A.; Bein, T. Excited-state dynamics in fully conjugated 2D covalent organic fameworks. *J. Am. Chem. Soc.* **2019**, *141*, 11565–11571.

23 Ding, H.; Li, J.; Xie, G.; Lin, G.; Chen, R.; Peng, Z.; Yang, C.; Wang, B.; Sun, J.; Wang, C. An AIEgen-based 3D covalent oganic framework for white light-emitting diodes. *Nat. Commun.* **2018**, *9*, 5234.

24 Li, X.; Wang, H.; Chen, H.; Zheng, Q.; Zhang, Q.; Mao, H.; Liu, Y.; Cai, S.; Sun, B.; Dun, C.; Gordon, M. P.; Zheng, H.; Reimer, J. A.; Urban, J. J.; Ciston, J.; Tan, T.; Chan, E. M.; Zhang, J.; Liu, Y. Dynamic covalent synthesis of crystalline porous graphitic frameworks. *Chem* **2020**, *6*, 933–944.

25 Zhang, Q.; Dong, S.; Shao, P.; Zhu, Y.; Mu, Z.; Sheng, D.; Zhang, T.; Jiang, X.; Shao, R.; Ren, Z.; Xie, J.; Feng, X.; Wang, B. Covalent organic framework-based porous ionomers for high performance fuel cells. *Science* **2022**, *378*, 181–186.

26 Yang, X.; Hu, Y.; Dunlap, N.; Wang, X.; Huang, S.; Su, Z.; Sharma, S.; Jin, Y.; Huang, F.; Wang, X.; Lee, S. H.; Zhang, W. A truxenone-based covalent organic framework as an all-solid-state lithium-ion battery cathode with high capacity. *Angew. Chem. Int. Ed.* **2020**, *59*, 20385–20389.

27 Wu, C.; Liu, Y.; Liu, H.; Duan, C.; Pan, Q.; Zhu, J.; Hu, F.; Ma, X.; Jiu, T.; Li, Z.; Zhao, Y. Highly conjugated three-dimensional covalent organic frameworks based on spirobifluorene for perovskite solar cell enhancement. *J. Am. Chem. Soc.* **2018**, *140*, 10016–10024.

28 Evans, A. M.; Parent, L. R.; Flanders, N. C.; Bisbey, R. P.; Vitaku, E.; Kirschner, M. S.; Schaller, R. D.; Chen, L. X.; Gianneschi, N. C.; Dichtel, W. R. Seeded growth of single-crystal two-dimensional covalentorganic frameworks. *Science* **2018**, *361*, 52–57.

29 Zhou, Z. B.; Sun, H. H.; Qi, Q. Y.; Zhao, X. Gradually tuning the flexibility of two-dimensional covalent organic frameworks via stepwise structural transformation and their flexibility-dependent properties. *Angew. Chem. Int. Ed.* **2023**, *62*, e202305131.

30 Li, L.; Yun, Q.; Zhu, C.; Sheng, G.; Guo, J.; Chen, B.; Zhao, M.; Zhang, Z.; Lai, Z.; Zhang, X.; Peng, Y.; Zhu, Y.; Zhang, H. Isoreticular series of two-dimensional covalent organic frameworks with the kgd topology and controllable micropores. *J. Am. Chem. Soc.* **2022**, *144*, 6475–6482.

31 Bi, S.; Zhang, Z.; Meng, F.; Wu, D.; Chen, J. S.; Zhang, F. Heteroatom-embedded approach to vinylene-linked covalent organic frameworks with isoelectronic structures for photoredox catalysis. *Angew. Chem. Int. Ed.* **2022**, *61*, e202111627.

32 Yang, G. H.; Zheng, Z.; Yin, C. C.; Shi, X. S; Wang, Y. Morphology engineering for covalent organic frameworks (COFs) by surfactant mediation and acid adjustment. *Chinese J. Polym. Sci.* **2022**, *40*, 338–344.

33 Gui, B.; Lin, G.; Ding, H.; Gao, C.; Mal, A.; Wang, C. Three-dimensional covalent organic frameworks: from topology design to applications. *Acc. Chem. Res.* **2020**, *53*, 2225–2234.

34 Guan, X.; Chen, F.; Fang, Q.; Qiu, S. Design and applications of three dimensional covalent organic frameworks. *Chem. Soc. Rev.* **2020**, *49*, 1357–1384.

35 El-Kaderi, H. M.; Hunt, J. R.; Mendoza-Cortés, J. L.; Côté, A. P.; Taylor, R. E.; O'Keeffe, M.; Yaghi, O. M. Designed synthesis of 3D covalent organic frameworks. *Science* **2007**, *316*, 268–272.

36 Gao, C.; Li, J.; Yin, S.; Lin, G.; Ma, T.; Meng, Y.; Sun, J.; Wang, C. Isostructural three-dimensional covalent organic frameworks. *Angew. Chem. Int. Ed.* **2019**, *58*, 9770–9775.

37 Ma, T.; Kapustin, E. A.; Yin, S. X.; Liang, L.; Zhou, Z.; Niu, J.; Li, L. H.; Wang, Y.; Su, J.; Li, J.; Wang, X.; Wang, W. D.; Wang, W.; Sun, J.; Yaghi, O. M. Single crystal X-ray diffraction structures of covalent organic frameworks. *Science* **2018**, *361*, 48–52.

38 Liu, Y.; Chen, P.; Wang, Y.; Suo, J.; Ding, J.; Zhu, L.; Valtchev, V.; Yan, Y.; Qiu, S.; Sun, J.; Fang, Q. Design and synthesis of a zeolitic organic framework. *Angew. Chem. Int. Ed.* **2022**, *61*, e202203584.

39 Xu, H.; Luo, Y.; See, P. Z.; Li, X.; Chen, Z.; Zhou, Y.; Zhao, X.; Leng, K.; Park, I.; Li, R.; Liu, C.; Chen, F.; Xi, S.; Sun, J.; Loh, K. P. Divergent chemistry paths for 3D and 1D metallo-covalent organic frameworks (COFs). *Angew. Chem. Int. Ed.* **2020**, *59*, 11527–11532.

40 Lin, G.; Ding, H.; Yuan, D.; Wang, B.; Wang, C. A pyrene-based, fluorescent three-dimensional covalent organic framework. *J. Am. Chem. Soc.* **2016**, *138*, 3302–3305.

41 Furukawa, H.; Yaghi, O. M. Storage of hydrogen, methane, and carbon dioxide in highly porous covalent organic frameworks for clean energy applications. *J. Am. Chem. Soc.* **2009**, *131*, 8875–8883.

42 Meng, Y.; Luo, Y.; Shi, J.; Ding, H.; Lang, X.; Chen, W.; Zheng, A.; Sun, J.; Wang, C. 2D and 3D Porphyrinic covalent organic frameworks: the influence of dimensionality on functionality. *Angew. Chem. Int. Ed.* **2020**, *59*, 3624–3629.

43 Xie, Y.; Li, J.; Lin, C.; Gui, B.; Ji, C.; Yuan, D.; Sun, J.; Wang, C. Tuning the topology of three-dimensional covalent organic frameworks *via* steric control: from pts to unprecedented Ijh. *J. Am. Chem. Soc.* **2021**, *143*, 7279–7284.

44 Ma, X.; Scott, T. F. Approaches and challenges in the synthesis of three-dimensional covalent-organic frameworks. *Commun. Chem.* **2018**, *1*, 98.

45 Guo, Z.; Zhan, Z.; Sun, J. Topological analysis and structural determination of three-dimensional covalent organic frameworks. *Adv. Mater.* **2024**, DOI: 10.1002/adma.202312889.

46 Gao, C.; Li, J.; Yin, S.; Sun, J.; Wang, C. Twist building blocks from planar to tetrahedral for the synthesis of covalent organic frameworks. *J. Am. Chem. Soc.* **2020**, *142*, 3718–3723.

47 Gui, B.; Xin, J.; Cheng, Y.; Zhang, Y.; Lin, G.; Chen, P.; Ma, J. X.; Zhou, X.; Sun, J.; Wang, C. Crystallization of dimensional isomers in covalent organic frameworks. *J. Am. Chem. Soc.* **2023**, *145*, 11276–11281.

48 Ji, C.; Su, K.; Wang, W.; Chang, J.; El-Sayed, E. M.; Zhang, L.; Yuan, D. Tunable cage-based three-dimensional covalent organic frameworks. *CCS Chem.* **2022**, *4*, 3095–3105.

49 Zhu, Q.; Wang, X.; Clowes, R.; Cui, P.; Chen, L.; Little, M. A.; Cooper, A. I. 3D Cage COFs: A dynamic three-dimensional covalent organic framework with high-connectivity organic cage nodes. *J. Am. Chem. Soc.* **2020**, *142*, 16842–16848.

50 Li, H.; Ding, J.; Guan, X.; Chen, F.; Li, C.; Zhu, L.; Xue, M.; Yuan, D.; Valtchev, V.; Yan, Y.; Qiu, S.; Fang, Q. Three-dimensional large-pore covalent organic framework with stp topology. *J. Am. Chem. Soc.* **2020**, *142*, 13334–13338.

51 Yin, Y.; Zhang, Y.; Zhou, X.; Gui, B.; Cai, G.; Sun, J.; Wang, C. Single-crystal three-dimensional covalent organic framework constructed from 6-connected triangular prism node. *J. Am. Chem. Soc.* **2023**, *145*, 22329–22334.

52 Liu, W.; Wang, K.; Zhan, X.; Liu, Z.; Yang, X.; Jin, Y.; Yu, B.; Gong, L.; Wang, H.; Qi, D.; Yuan, D.; Jiang, J. Highly connected three-dimensional covalent organic framework with flu topology for high-performance Li-S batteries. *J. Am. Chem. Soc.* **2023**, *145*, 8141−8149.
53 Gropp, C.; Ma, T.; Hanikel, N.; Yaghi, O. M. Design of higher valency in covalent organic frameworks. *Science* **2020**, *370*, eabd6406.
54 Carlucci, L.; Ciani, G.; Proserpio, D. M.; Mitina, T. G.; Blatov, V. A. Entangled two-dimensional coordination networks: a general survey. *Chem. Rev.* **2014**, *114*, 7557−7580.
55 Jin, F.; Nguyen, H. L.; Zhong, Z.; Han, X.; Zhu, C.; Pei, X.; Ma, Y.; Yaghi, O. M. Entanglement of square nets in covalent organic frameworks. *J. Am. Chem. Soc.* **2022**, *144*, 1539−1544.
56 Cheng, Y.; Xin, J.; Xiao, L.; Wang, X.; Zhou, X.; Li, D.; Gui, B.; Sun, J.; Wang, C. A fluorescent three-dimensional covalent organic famework formed by the entanglement of two-dimensional sheets. *J. Am. Chem. Soc.* **2023**, *145*, 18737−18741.
57 Xiao, Y.; Ling, Y.; Wang, K.; Ren, S.; Ma, Y.; Li, L. Constructing a 3D covalent organic framework from 2D hcb nets through inclined interpenetration. *J. Am. Chem. Soc.* **2023**, *145*, 13537−13541.
58 Wan W.; Sun, J.; Su, J.; Hovmoller, S.; Zou, X. Three-dimensional rotation electron diffraction: software RED for automated data collection and data processing. *J. Appl. Crystallogr.* **2013**, *46*, 1863−1873.
59 Kabsch, W. Integration, scaling, space-group assignment and post-refinement. *Acta Crystallogr. D* **2010**, *66*, 133−144.

https://doi.org/10.1007/s10118-024-3133-5